Direct measurements of anode/cathode gap plasma in cylindrically imploding loads on the Z machine

A. Porwitzky, D. H. Dolan, M. R. Martin, G. Laity, R. W. Lemke, and T. R. Mattsson

Citation: Physics of Plasmas **25**, 063110 (2018); doi: 10.1063/1.5026225
View online: https://doi.org/10.1063/1.5026225
View Table of Contents: http://aip.scitation.org/toc/php/25/6
Published by the American Institute of Physics

Direct measurements of anode/cathode gap plasma in cylindrically imploding loads on the Z machine

A. Porwitzky,[a] D. H. Dolan, M. R. Martin, G. Laity, R. W. Lemke, and T. R. Mattsson
Sandia National Laboratories, Albuquerque, New Mexico 87185, USA

(Received 16 February 2018; accepted 28 May 2018; published online 12 June 2018)

By deploying a photon Doppler velocimetry based plasma diagnostic, we have directly observed low density plasma in the load anode/cathode gap of cylindrically converging pulsed power targets. The arrival of this plasma is temporally correlated with gross current loss and subtle power flow differences between the anode and the cathode. The density is in the range where Hall terms in the electromagnetic equations are relevant, but this physics is lacking in the magnetohydrodynamics codes commonly used to design, analyze, and optimize pulsed power experiments. The present work presents evidence of the importance of physics beyond traditional resistive magnetohydrodynamics for the design of pulsed power targets and drivers. https://doi.org/10.1063/1.5026225

The Z machine (Z) at Sandia National Laboratories has been successfully utilized for many years as a platform for exploring high energy density states of matter.[1–6] In the last few years, interest has grown in understanding the detailed power flow physics of Z to best design future pulsed power drivers that could potentially deliver over 30 MA of current to target loads.[7] Identifying and understanding all loss mechanisms in Z is recognized as a critical step along the path to the next generation of pulsed power drivers designed to reach ignition and high-yield fusion. In this letter, we present new direct evidence of a current loss mechanism and simulations at a higher level of theory complementing the experimental data.

Cylindrically convergent load geometries are being exploited for both inertial confinement fusion (ICF) and dynamic material properties (DMP) experiments on Z due to the high pressures they can achieve.[4–6,8] In a cylindrically convergent geometry, the current enters the bottom of the load and flows along the inner surface of a cylindrical anode, typically composed of aluminum or beryllium. The current then passes across a short at the top of the load to reach the cathode, where it then flows down the outside of that surface back into Z. The magnetic field established in the anode/cathode (AK) gap causes the cathode to implode, while the anode explodes at much lower velocity due to the difference in field strength and liner mass. If spatially and temporally resolved velocimetry measurements are taken on the outer/inner surface of the anode/cathode, then that velocity can be used in a multiphysics simulation to determine the drive current that resulted in conductor motion.[8,9] Solving this inverse problem—where an initial guess load current is adjusted via a non-linear solver until a multiphysics simulation produces the measured velocity response—is colloquially referred to as "unfolding a current." Figure 1 shows a schematic of the generic load geometry used in the experiments presented. Photon Doppler Velocimetry[10] (PDV) is used to measure the imploding cathode surface velocity at three angular locations through a configuration similar to that outlined in Ref. 11, with the multiple angular locations enabling an estimate of the uniformity of the implosion. Either PDV or velocity interferometer system for any reflector[12] (VISAR) is suitable for measuring anode motion, a measurement that is ideally performed at multiple angular locations in order to estimate target concentricity.[9] All PDV/VISAR probes on Z are temporally correlated with machine time with sub-nanosecond accuracy; thus, all unfolded currents are temporally synchronized to each other.

Prior work (Ref. 8) indicated that cylindrical current unfolds are remarkably sensitive to minor current fluctuations. For an imploding cathode of initial outer radius R, the magnetic pressure on its drive surface is given as

$$P_B = \frac{\mu_o I^2}{8\pi^2 R^2},$$

where μ_o is the permeability of free space, and I is the total electric current supplied to the load. We can see that at the smaller cathode radius its outer surface experiences a much higher pressure than does the anode inner surface. The prior work first reported a deviation between anode and cathode currents that precluded utilizing the anode current to calculate a material equation of state (EOS) at high pressure. It was theorized that the cause could be an unaccounted for aluminum solid-solid phase transition at high pressure that would affect the aluminum cathode. A subsequent experiment using a copper cathode exhibited the same current deviation at the same temporal location, indicating that the cause was not the material models being employed.

Experiments on Z and other pulsed power facilities are currently designed using computational multiphysics codes that employ the resistive magnetohydrodynamic (MHD) system of equations. A hypothesis for the current discrepancy is that the total current is not confined to the cathode liner, as predicted by MHD simulation; a small fraction of the current

[a]Electronic mail: ajporwi@sandia.gov

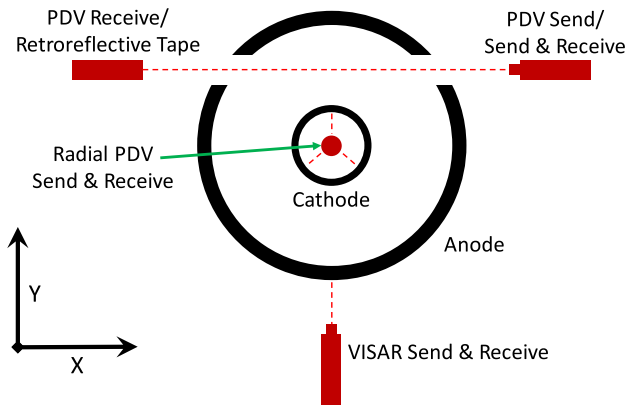

FIG. 1. Schematic of the geometry used on the cylindrical implosion experiments presented in this letter.

is carried by an unaccounted for low density plasma in the AK gap. Consequently, computational unfolds of the total load current using velocimetry measurements and MHD yield slightly less current for the cathode than the anode. The Perseus Extended-MHD[13] code incorporates Hall terms in the MHD approximation, allowing for the effects of low density plasmas to be captured. Perseus was used to simulate a cylindrical implosion, whereby it was observed that low density plasmas generated by ohmic heating upstream of the load (or in the load itself) are preferentially driven to the cathode surface by the global magnetic field gradient. Figure 2 shows atomic number density along a line extending from inside the cathode to a point just inside the anode in the cylindrical implosion simulation. These data, taken late in time after liner motion, illustrate the difference between Perseus results in Extended-MHD and MHD (with and without Hall terms).

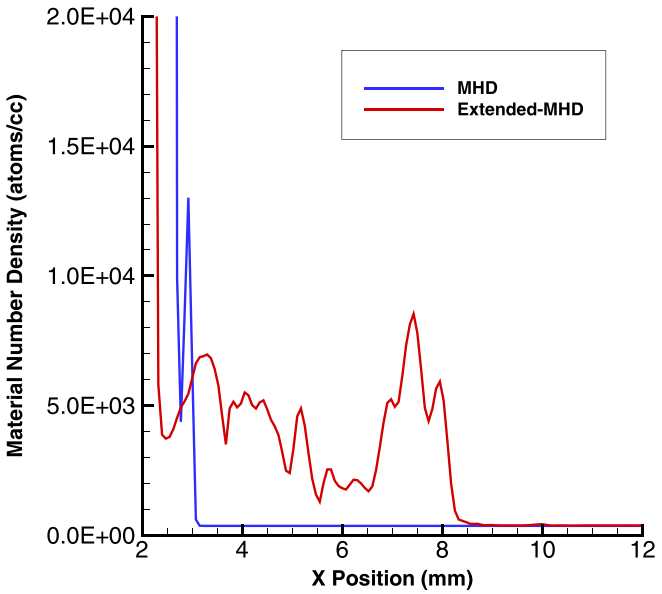

FIG. 2. Comparison of material number density along a line extending from inside the cathode radially into the AK gap in a cylindrical implosion calculation using the Perseus code in both MHD and Extended-MHD formulations. A significant buildup of low density plasma is apparent in the region surrounding the cathode that extends significantly into the AK gap in the Extended-MHD case. The MHD case shows the typical low density blowoff confined to the liner surface.

There is a significant buildup of low density plasma surrounding the cathode (represented as the vertical lines around 3 mm) in the Extended-MHD case, which can be seen to alter the liner dynamics as the Extended-MHD case has imploded to a smaller outer radius than the MHD case. Our calculations indicate that if this plasma carries 1% of the load current, then the deviations seen in Ref. 8 can be accounted for by this mechanism.

In order to experimentally investigate the current loss, we deployed a chordal PDV array as illustrated in Fig. 1 to measure the index of refraction changes along the beam path. PDV measures apparent velocity (v^*) along a laser beam path by relating the time varying index of refraction (n) to a Doppler shift via

$$v^*(t) = -\frac{d}{dt}\int n(x,t)\,dx.$$

Note that for an electron plasma we expect dn/dt to decrease over time; thus, we anticipate a positive velocity change. If any material were to enter the vacuum AK gap, then the chordal PDV would return a "velocity" outside of the background noise, which for the Z PDV system is approximately ± 10 m/s.[14] The chordal PDV can be regarded as an elaborate laser break screen for detecting low density plasma in a vacuum environment. Further details of this system are presented in Ref. 15. For the experiments presented here, two or three PDV send/receive probes were stacked vertically ($\hat{z}$) along the AK gap allowing for rough transit time estimates to be made. If material were to enter from upstream of the load, we would expect the bottom probe to report an index of refraction change before the top probe. Figure 1 shows two configurations for the chordal PDV: one using an opposed receive fiber and the other employing retroreflective tape to bounce the probe beam back to the co-aligned receive fiber in the send probe. The retroreflective tape was employed because of the difficulty in aligning the micron scale fibers over a distance of 1–2 cm although this was achieved on one of our experiments. The analysis and conclusions are not changed by this difference although in the case of the retroreflective tape the beam path length is twice that of the receive fiber case.

Figure 3 shows the results of Z2964 and Z3022, immediate follow-on experiments to the one discussed in Ref. 8. Each of these experiments used 450 μm thick aluminum anodes of 13 mm inner radius and 847 μm thick copper cathodes of inner radius 2.1 mm. Target metrology for all the experiments discussed here indicate variances of 1–2 μm in both radius and thickness, which is typical for Z target loads of this type. Z3022 was the first experiment to deploy the chordal PDV diagnostic although cathode velocity was not returned. Z3022 anode current matches Z2964 anode current to within unfold uncertainty; thus, a comparison can safely be made. The previously observed anode/cathode current deviation occurs at 2.8 μs. Cathode implosion results in a loss of velocimetry data and thus the unfolding of the drive current cannot be carried past 2.875 μs. Although visually small, this difference is outside the unfold uncertainty, which is dominated by the anode and is estimated to be less than

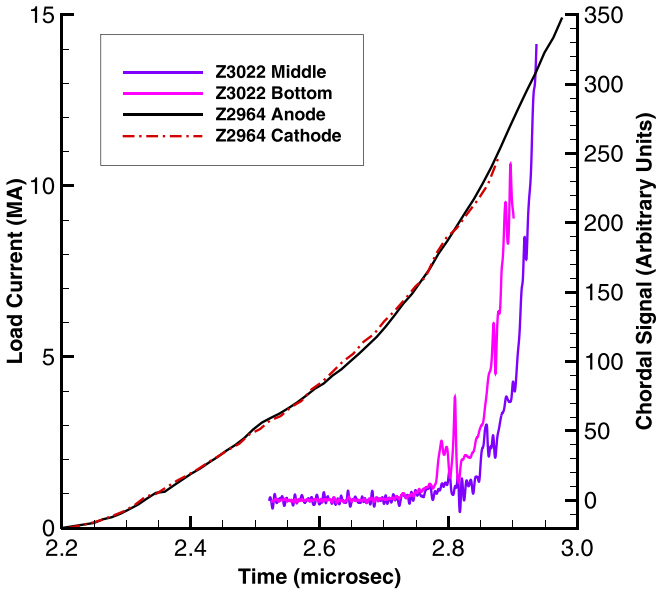

FIG. 3. Z2964 load current inferred from velocimetry data for anode and cathode liners overlaid with PDV plasma diagnostic signals from Z3022 illustrating that deviation occurs as plasma enters the AK gap from upstream of the load at approximately 2.8 μs.

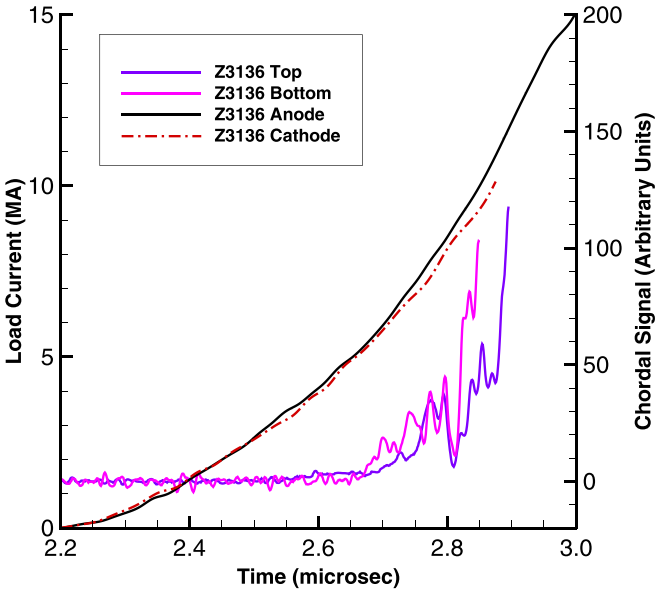

FIG. 4. Z3136 velocimetry inferred currents and chordal plasma diagnostic data demonstrating that early onset plasma generation results in earlier anode/cathode current deviation.

$\pm$150 kA at the time of current deviation. It is worth noting that a qualitatively similar current deviation occurs around 2.7 μs; however, this is due to uncertainty in the anode unfold, which is higher at lower current loads.[9] Z3022 employed three chordal PDVs vertically separated 5 mm from each other in the retroreflective configuration although the top PDV did not return data due to a probe failure. Plasma appears to be entering from upstream of the load and flowing in the $+\hat{z}$ direction.

In order to verify that low density plasma ablating from the power flow surfaces is responsible for the deflection observed in Z2964/Z3022, the load hardware was modified to incorporate additional 90° corners on power flow surfaces just upstream of the load. These extra corners should increase plasma generation when carrying multiple mega-amp current loads. All anode/cathode materials and dimensions were left unchanged. The results of this experiment (Z3136) are shown in Fig. 4. Z3136 deployed two chordal PDVs, equivalent to the bottom and top positions on Z3022, with the middle location replaced by an unrelated diagnostic. The low density plasma arrives 0.1 μs earlier in Z3136, resulting in a more significant anode/cathode current deviation by the time of cathode implosion.

These results demonstrate that the previously observed anode/cathode current deviations are due to low density plasma in the load AK gap. The effect is significant and has not been previously diagnosed. This plasma carries a portion of the total load current, diffusing it away from the cathode surface, altering how the magnetic force couples to the cathode, effectively decreasing the force applied and thus decreasing the inferred current.

The experiments thus far discussed utilized the same 800 ns rise to 15 MA current pulse intended to isentropically compress the cathode. The majority of cylindrically imploding experiments on Z utilize a 100 ns rise to 20+ MA current pulse meant to implode the cathode as rapidly as possible to achieve pressures sufficient for nuclear fusion conditions. In these experiments, the voided cathode interior housing the radial PDV is instead filled with a fusion fuel of some type, such as in the MagLIF concept.[4–6] Z3084 deployed the chordal PDV to monitor low density plasma arrival on a short pulse experiment and utilized two probes of the receive fiber configuration spaced 4 mm apart in $\hat{z}$. For this experiment, the cathode was 400 μm thick aluminum with an inner radius of 3.0 mm, with the anode identical to the previous experiments. As expected, the cathode liner shocked during implosion; thus, a meaningful cathode current cannot be inferred in this case. Insight can be gained by comparing a loss-less load current prediction from the Z circuit model[16] to the unfolded anode current (Fig. 5). The negative chordal PDV signal before the spike is believed to be due to a radiation effect causing the index of refraction in the PDV fiber to momentarily increase.[15] Most interesting is that the aggressive arrival of plasma in the load AK gap coincides with the onset of the primary current loss mechanism.

The chordal plasma diagnostic makes it clear that low density plasma in the load AK gap affects the dynamics of all cylindrical liner implosions on Z, and likely on all pulsed power drivers. Moreover, the implication from the short pulse experiment (Z3084) is that this plasma is a key player in load current losses. We are careful to not assert any hypothesis as to the source of this plasma. We also do not claim that the current loss indicated in Fig. 5 is a result of this plasma, merely that they are co-timed. It is possible that convolute losses are generating plasma that flows along the AK gap into the load region, and indeed the timing between the two probes indicates that the short pulse plasma is traveling at much higher velocity than in the long pulse case. Various modeling efforts are underway to attempt to identify possible sources of this plasma, with theories predominantly focused on convolute electron losses, contaminant desorption from

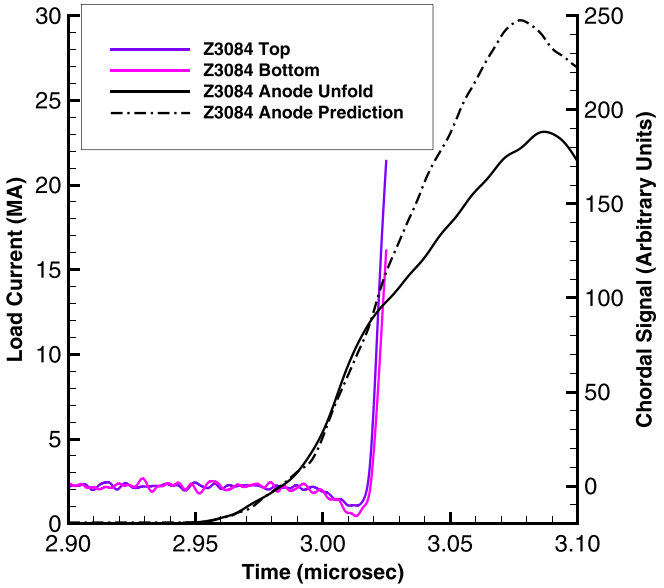

FIG. 5. Z3084 velocimetry inferred anode current and chordal plasma diagnostic data demonstrating that for short pulse loads the plasma arrives more aggressively, temporally coinciding with the major current loss mechanism.

power flow surfaces, and low density metallic vaporization under joule heating.

For a known chordal PDV laser path length (L), we can approximately relate the apparent velocity to the average refractive index along the path length ($\hat{n}$) as

$$v^*(t) \approx -L\frac{d\hat{n}}{dt},$$

which allows us to integrate the "velocity" returned by the chordal PDV into a plasma density under the assumption that the observed plasma is comprised exclusively of free electrons (if it is not, then ion refractive index change could counter some electron index change). This yields the approximate plasma densities at cutoff given in Table I for each of the experiments discussed here. We consider this plasma density to be an order-of-magnitude estimate. The PDV laser employed operated at 1550 nm, for which the critical density for plasma opacity is 4.6e20 electrons/cc. We see from Table I that signal cutoff occurs well below the critical density. One possible explanation is beam deflection; as the index of refraction increases, the laser beam is deflected outside the aperture of the receive fiber. Another explanation is that the density is calculated based on the mean index of refraction along the path length L; if a localized puff of plasma with density just below the critical density were to cross the PDV beam, then we would infer a density well below the real density by averaging. Similarly, if the puff was above the critical density, we would infer a density well below that just before cutoff.

TABLE I. Peak plasma densities (electron/cc) at signal cutoff for each of the experiments presented. The critical density for 1550 nm light is 4.6e20 electron/cc.

Z2964/Z3022 (baseline)	Z3136 (extra corners)	Z3084 (short pulse)
23e16	7e16	15e16

With these order-of-magnitude number densities, we can estimate the importance of the Hall terms neglected in MHD codes. With some manipulation, the generalized Ohm's law can be rewritten[17] as

$$\vec{J} + \frac{|\Omega_e|}{\nu_c}\left(\vec{J} \times \frac{\vec{B}}{B}\right) = \sigma\vec{E}^*,$$

where $\vec{E}^*$ is an effective electric field which includes the electron inertial term and $\vec{v} \times \vec{B}$ drift, $\vec{J}$ is the electric current density, σ is the scalar electrical conductivity, $\Omega_e = eB/m_e$ is the electron cyclotron frequency, and ν_c is the collision frequency. Hall physics is represented by the $\vec{J} \times \vec{B}$ term, and we can see that the traditional MHD Ohm's law is recovered from the above if $|\Omega_e| \ll \nu_c$. We now use values from the above density estimates and Perseus simulations, selecting those that will give the smallest ratio of $|\Omega_e|/\nu_c$. Thus, we take $B = 100$ T, electron temperature $T_e = 1$ eV, and an electron number density of 1e17 electron/cc, for which we find $|\Omega_e|/\nu_c \sim 100$. This ratio will increase if B increases ($B = 1000$ T near the cathode), if T_e increases (which is predicted by Perseus), or if electron density decreases (a regime observed by the PDV plasma diagnostic). We conclude that the low density plasma we have detected is undoubtedly impacted by Hall dynamics.

Low density plasma has been consistently detected in the AK gap of cylindrically imploding loads on Z. Due to the extreme sensitivity of the cylindrical DMP platform, the effect of this plasma diffusing a small fraction of the load current away from the imploding cathode liner has been confirmed on multiple experiments. This plasma—which is not present under the MHD assumption—is having a measurable effect on Z load configurations, which are designed using computational codes based on the MHD assumption. The chordal PDV configuration has demonstrated that future codes—used to design not only load hardware, but also the next generation pulsed power drivers—need to incorporate Extended-MHD physics in order to accurately predict load response. The cylindrical DMP platform will continue to be a valuable power flow diagnostic far into the future. Efforts are underway to explore, characterize, source, and mitigate this low density plasma. We expect these findings to stimulate research in the role of low density plasma in current loss mechanisms as well as drive the development of Extended-MHD formulation codes for pulsed power physics.

We sincerely thank the staff, technologists, and management who made the experiments on Z possible. We would also like to thank Professor Charles Seyler at Cornell for his contributions to the low density plasma/Perseus work. This work was supported by the NNSA Science and Inertial Confinement Fusion programs. Sandia National Laboratories is a multi-mission laboratory managed and operated by the National Technology and Engineering Solutions of Sandia LLC, a wholly owned subsidiary of Honeywell International Inc. for the U.S. Department of Energy's National Nuclear Security Administration under Contract No. DE-NA0003525.

[1]J.-P. Davis, C. Deeney, M. D. Knudson, R. W. Lemke, T. D. Pointon, and D. E. Bliss, "Magnetically driven isentropic compression to multimegabar pressures using shaped current pulses on the z accelerator," Phys. Plasmas **12**, 056310 (2005).
[2]J. Davis and M. D. Knudson, "Multimegabar measurement of the principal quasi isoentrope for tantalum," AIP Conf. Proc. **1195**, 673–676 (2009).
[3]S. Root, L. Shulenburger, R. W. Lemke, D. H. Dolan, T. R. Mattsson, and M. P. Desjarlais, "Shock response and phase transitions of MgO at planetary impact conditions," Phys. Rev. Lett. **115**, 198501 (2015).
[4]R. D. McBride, S. A. Slutz, C. A. Jennings, D. B. Sinars, M. E. Cuneo, M. C. Herrmann, R. W. Lemke, M. R. Martin, R. A. Vesey, K. J. Peterson, A. B. Sefkow, C. Nakhleh, B. E. Blue, K. Killebrew, D. Schroen, T. J. Rogers, A. Laspe, M. R. Lopez, I. C. Smith, B. W. Atherton, M. Savage, W. A. Stygar, and J. L. Porter, "Penetrating radiography of imploding and stagnating beryllium liners on the z accelerator," Phys. Rev. Lett. **109**, 135004 (2012).
[5]M. R. Gomez, S. A. Slutz, A. B. Sefkow, D. B. Sinars, K. D. Hahn, S. B. Hansen, E. C. Harding, P. F. Knapp, P. F. Schmit, C. A. Jennings, T. J. Awe, M. Geissel, D. C. Rovang, G. A. Chandler, G. W. Cooper, M. E. Cuneo, A. J. Harvey-Thompson, M. C. Herrmann, M. H. Hess, O. Johns, D. C. Lamppa, M. R. Martin, R. D. McBride, K. J. Peterson, J. L. Porter, G. K. Robertson, G. A. Rochau, C. L. Ruiz, M. E. Savage, I. C. Smith, W. A. Stygar, and R. A. Vesey, "Experimental demonstration of fusion-relevant conditions in magnetized liner inertial fusion," Phys. Rev. Lett. **113**, 155003 (2014).
[6]S. A. Slutz and R. A. Vesey, "High-gain magnetized inertial fusion," Phys. Rev. Lett. **108**, 025003 (2012).
[7]G. Laity, C. Aragon, D. Dolan, R. Falcon, M. Gomez, M. Hess, B. Hutsel, C. Jennings, M. Johnston, D. Lamppa, S. Patel, A. Porwitzky, P. VanDevender, T. Webb, G. Rochau, W. Stygar, and M. Cuneo, "Experimental platform development for studying vacuum power flow physics at the Sandia Z accelerator," in *2017 IEEE Pulsed Power Conference, 2017*.
[8]R. W. Lemke, D. H. Dolan, D. G. Dalton, J. L. Brown, K. Tomlinson, G. R. Robertson, M. D. Knudson, E. Harding, A. E. Mattsson, J. H. Carpenter, R. R. Drake, K. Cochrane, B. E. Blue, A. C. Robinson, and T. R. Mattsson, "Probing off-Hugoniot states in Ta, Cu, and Al to 1000 GPa compression with magnetically driven liner implosions," J. Appl. Phys. **119**, 015904 (2016).
[9]A. Porwitzky and J. Brown, "Uncertainties in cylindrical anode current inferences on pulsed power drivers," Phys. Plasmas **25**, 063102 (2018).
[10]O. T. Strand, D. R. Goosman, C. Martinez, T. L. Whitworth, and W. W. Kuhlow, "Compact system for high-speed velocimetry using heterodyne techniques," Rev. Sci. Instrum. **77**, 083108 (2006).
[11]D. Dolan, R. Lemke, R. McBride, M. Martin, E. Harding, D. Dalton, B. Blue, and S. Walker, "Tracking an imploding cylinder with photonic Doppler velocimetry," Rev. Sci. Instrum. **84**, 55102 (2013).
[12]L. M. Barker and R. E. Hollenbach, "Laser interferometer for measuring high velocities of any reflecting surface," J. Appl. Phys. **43**, 4669–4675 (1972).
[13]C. E. Seyler and M. R. Martin, "Relaxation model for extended magneto-hydrodynamics: Comparison to magnetohydrodynamics for dense z-pinches," Phys. Plasmas **18**, 012703 (2011).
[14]D. H. Dolan, "Accuracy and precision in photonic Doppler velocimetry," Rev. Sci. Instrum. **81**, 053905 (2010).
[15]D. H. Dolan, K. Bell, B. Fox, S. C. Jones, P. Knapp, M. R. Gomez, M. Martin, A. Porwitzky, and G. Laity, "Plasma and radiation detection via fiber interferometry," J. Appl. Phys. **123**, 034502 (2018).
[16]B. T. Hutsel, J. P. Davis, R. B. Campbell, W. E. Fowler, H. L. Hanshaw, C. Jennings, M. Jones, R. W. Lemke, F. W. Long, M. R. Lopez, G. R. McKee, J. K. Moore, J. L. Porter, M. E. Savage, M. E. Sceiford, W. A. Stygar, P. A. Corcoran, B. A. Whitney, A. R. Camacho, D. Hinshelwood, and T. C. Wagoner, "Z machine circuit model development," in *2013 Abstracts IEEE International Conference on Plasma Science (ICOPS)* (2013), pp. 1.
[17]T. J. M. Boyd and J. J. Sanderson, *The Physics of Plasmas* (Cambridge University Press, 2003).